



Performances of metal fluoride added carbon anodes with pre-electrolysis for electrolytic synthesis of NF_3

Tomohiro Isogai^{a,d}, Kazuhiro Hirooka^a, Tetsuro Tojo^c, Hitoshi Takebayashi^c,
Morihiro Saito^b, Minoru Inaba^{a,b,1}, Akimasa Tasaka^{a,b,*,1}

^a Department of Applied Chemistry, Graduate School of Engineering, Doshisha University, 1-3 Miyakodani, Tatara, Kyotanabe, Kyoto 610-0321, Japan

^b Department of Molecular Chemistry and Biochemistry, Faculty of Science and Engineering, Doshisha University, 1-3 Miyakodani, Tatara, Kyotanabe, Kyoto 610-0321, Japan

^c Advanced Carbon Technology Center, Toyo Tanso Co., Ltd., 5-7-12 Takeshima, Nishiyodogawa-ku, Osaka 555-0011, Japan

^d Process Technology Department, Chemical Division, Daikin Industries, Ltd., 1-1 Nishihitotsuya, Settsu, Osaka 566-8585, Japan

ARTICLE INFO

Article history:

Received 3 August 2010

Received in revised form 10 October 2010

Accepted 16 October 2010

Available online 28 March 2011

Keywords:

Nitrogen trifluoride

Metal fluoride added carbon anode

Fluorine-graphite intercalation compounds

Semi-covalent C–F bond

Graphite fluoride

ABSTRACT

Metal fluoride added carbon anodes treated by pre-electrolysis were investigated for electrolytic production of nitrogen trifluoride (NF_3) in molten $\text{NH}_4\text{F}\cdot\text{KF}\cdot 4\text{HF}$ at 100°C . The conditions for pre-electrolysis were first optimized using a graphite sheet anode as a model anode. The formation of fluorine-graphite intercalation compounds (fluorine-GICs) with semi-covalent C–F bonds, $(\text{C}_x\text{F})_n$, on the MgF_2 and CaF_2 added carbon anode surface was accelerated by pre-electrolysis at potentials less than 4.0V. Critical current densities (CCD) on the MgF_2 added carbon anodes pre-electrolyzed under various conditions were determined, and the highest CCD was 290 mA cm^{-2} obtained for that pre-electrolyzed at 3.5 V for 500 C cm^{-2} . This anode was successfully used in the electrolysis at 100 mA cm^{-2} for 290 h and the maximum NF_3 current efficiency was 55%. From these results, it was concluded that the metal fluoride added carbon anode treated by pre-electrolysis has a high potential for electrolytic production of NF_3 at higher current density.

© 2010 Elsevier Ltd. All rights reserved.

1. Introduction

A large amount of nitrogen trifluoride (NF_3) is currently produced and consumed as a dry etchant and a cleaning gas for CVD processes in the electronic industry in Japan. Two methods are known for electrolytic production of NF_3 : One is the electrolysis of molten $\text{NH}_4\text{F}\cdot 2\text{HF}$ with nickel anode, and the other is the electrolysis of molten $\text{NH}_4\text{F}\cdot\text{KF}\cdot 4\text{HF}$ with carbon anode [1]. The former method has an advantage that pure NF_3 free from carbon tetrafluoride (CF_4) can be obtained. However, a relatively high corrosion rate of the nickel anode is critical problems, which raise the cost of NF_3 . On the other hand, the latter method using carbon anode is free from corrosion of the anode; however, it has drawbacks such as the occurrence of the anode effect, disintegration of the anode, and contamination of NF_3 with a small amount of CF_4 . Of these, the most serious problem of the latter method to be solved is the occurrence of the anode effect.

The anode effect is caused by formation of a graphite fluoride layer with covalent C–F bonds, $(\text{CF})_n$, which has a very low surface energy and reduces the effective surface area of the anode [2–5],

on the carbon surface. On the other hand, fluorine-graphite intercalation compounds (fluorine-GICs) with semi-covalent C–F bonds, $(\text{C}_x\text{F})_n$ ($x > 3$), which have a higher surface energy and a higher electric conductivity, are also formed on the carbon anode during electrolysis. It has been reported that the presence of fluorine-GICs on the carbon anode surface effectively suppresses the anode effect [2–25].

Because the formation of fluorine-GICs is catalyzed by metal fluorides such as LiF , AlF_3 , MgF_2 , NiF_2 and so on [15], several attempts using metal fluorides have been examined to suppress the anode effect for several decades. It has been reported that addition of metal fluorides into the melts is effective to suppress the anode effect [16–18]. However, the concentration of the additive near the anode surface decreases with time, because it progressively precipitates as sludge on the bottom of cell. Therefore, it is necessary to add the metal fluoride periodically into the electrolyte in order to maintain the concentration of the additive. Furthermore, the repetitive addition of the metal fluoride to the electrolyte spoils the performance of electrolysis because of an increase in the viscosity of the electrolyte, and needs frequent removal of the sludge from the bottom of cell. Groult et al. investigated detail the electrochemistry of modified carbon anodes prepared by impregnation with solutions containing a precursor salt, such as $\text{Al}(\text{NO}_3)_3$ and $\text{Ni}(\text{NO}_3)_2$ [7,11,12]. Furthermore, the LiF impregnated anodes are prepared by immersing into the pore of row carbon material into

* Corresponding author. Tel.: +81 774 65 6592; fax: +81 774 65 6841.

E-mail address: atasaka@mail.doshisha.ac.jp (A. Tasaka).

¹ ISE member.

molten LiF under high pressure employing Hot Isostatic Pressing Process. It has been reported to be much effective and useful than the addition of LiF into the electrolyte [20–25].

Recently, metal fluoride added carbon anodes were developed and investigated from viewpoints of surface energy and current efficiency for NF_3 production in molten $\text{NH}_4\text{F-KF-HF}$ systems [26]. The results indicated that metal fluoride added carbon anodes are successfully used in the electrolysis at 10 mA cm^{-2} for 200 h and the maximum current efficiencies of NF_3 are almost equal to pristine carbon (Pristine-C) anode. In addition, it has been reported that pre-electrolysis of a carbon anode at potentials lower than 2.3 V, where fluoride anions cannot discharge, is effective for forming fluorine-GICs with semi-covalent C–F bonds and results in an improvement of CCD [27,28].

In the present study, anodic behavior of MgF_2 and CaF_2 added carbon (MgF_2/C and CaF_2/C) anodes were studied in the $\text{NH}_4\text{F-KF-4HF}$ melt. The conditions for pre-electrolysis were first optimized using a graphite sheet anode as a model anode in the $\text{NH}_4\text{F-KF-3HF}$ melt containing MgF_2 or CaF_2 . The effects of the pre-electrolysis conditions, such as anode potential and charge passed, on the critical current density (CCD) on MgF_2/C anodes were investigated in the $\text{NH}_4\text{F-KF-4HF}$ melt. Electrolysis was then conducted in the $\text{NH}_4\text{F-KF-4HF}$ melt with the MgF_2/C anode treated with pre-electrolysis under the optimized condition.

2. Experimental

Molten fluorides of $\text{NH}_4\text{F-KF-4HF}$ and $\text{NH}_4\text{F-KF-3HF}$ were used as electrolytes. They were prepared from KF-HF (Morita Chemical Industries, 99.9%), $\text{NH}_4\text{F-HF}$ (Morita Chemical Industries, 99.9%), and extra pure anhydrous hydrogen fluoride (Morita Chemical Industries, 99.99%) in sealed nickel vessels.

In order to obtain the anodic polarization curves, MgF_2 (5 wt%) and CaF_2 (4 wt%) added isotropic dense carbons (MgF_2/C and CaF_2/C , Toyo Tanso Co., Ltd.) [26] and pristine isotropic dense carbon (Pristine-C, FE-5, Toyo Tanso Co., Ltd., density: 1.69 g cm^{-3} , porosity: 11.7 vol.%, flexural strength: 103 MPa) [20] with a surface area of 1.0 cm^2 were used as anodes. A nickel sheet with a surface area of ca. 40 cm^2 was used as a cathode and the $\text{NH}_4\text{F-KF-4HF}$ melt at 100°C was used as an electrolyte. A box-type cell made from PTFE (polytetrafluoroethylene) with a capacity of 0.8 dm^3 described in previous papers [27,29] was used.

In order to optimize the pre-electrolysis conditions, a graphite sheet (Toyo Tanso Co., Ltd.) with a surface area of 0.5 or 1.0 cm^2 was used as the anode. The nickel sheet with a surface area of ca. 60 cm^2 was used as the cathode. Here $\text{NH}_4\text{F-KF-3HF}$ melt at 100°C was used as an electrolyte instead of $\text{NH}_4\text{F-KF-4HF}$ melt in order to suppress the exfoliation of the graphite sheet anode during electrolysis. An excess amount of MgF_2 or CaF_2 (Sigma-Aldrich Corp.) was added in the electrolyte to be saturated. A beaker-type PTFE cell with a capacity of 0.3 dm^3 described in a previous paper [30] was used.

In order to investigate the CCDs and the current efficiency for NF_3 formation, MgF_2/C and the Pristine-C samples with a surface area of 10 cm^2 were used as anodes. A cylindrical nickel cell with a capacity of 1.5 dm^3 [29,31] was used. The anode was located at the center of the cell and the cell wall was utilized as the cathode. A surface area of cathode is not less than 300 cm^2 . The $\text{NH}_4\text{F-KF-4HF}$ melt at 100°C was used as an electrolyte.

A Cu/CuF_2 electrode ($402 \pm 3\text{ mV vs. H}_2$ at 100°C) was employed as a reference electrode in all electrochemical measurements [32], but the potentials are referred to as volts vs. the hydrogen electrode in the present study. The cells were placed in a dry nitrogen chamber to remove moisture from the atmosphere. Since the chemicals contained water to some extent, electrolysis for dehydration was conducted using an auxiliary carbon anode and the Ni counter electrode at ca. 10 mA cm^{-2} for about ten days to reduce the water

content to less than 0.02 wt% (ca. 20 mmol dm^{-3}) [33], prior to electrochemical measurements. Anodic polarization curves were obtained at a sweep rate of 200 mV s^{-1} using an automatic polarization system (Hokuto Denko Ltd., HZ-3000). The pre-electrolysis was conducted at a constant current density of 5 mA cm^{-2} or at constant potentials of 2.3, 3.5, 4.0, 6.0, and 8.0 V with a potentiostat/galvanostat HA-303 (Hokuto Denko Ltd.) and a coulomb meter HF-201 (Hokuto Denko Ltd.). The electrolytic productions of NF_3 were carried out galvanostatically at current densities in the range of $5\text{--}300\text{ mA cm}^{-2}$ with a potentiostat/galvanostat HA-303 (Hokuto Denko Ltd.).

XRD and XPS analyses were conducted using RINT-2500 (Rigaku Corp. Co., Ltd.) with $\text{Cu-K}\alpha$ radiation and using AXIS-165 (Shimadzu Corp. Co., Ltd.) with $\text{Mg-K}\alpha$ radiation (1253.6 eV), respectively. For XPS measurements, gold thin film was vapor-deposited on the sample, and the binding energy of the gold $4f_{7/2}$ level at 84.0 eV was used for calibration. Raman spectra were obtained with a T-64000 spectrometer (Horiba Jobin Yvon Inc.) using an Ar^+ -ion laser (514.5 nm, 100 mW) as an excitation source. SEM images were obtained with a cold field emission scanning electron microscope S-4300 (Hitachi High-Technologies Corp.).

The anode gas was analyzed with a gas chromatograph/mass spectrometer (GCMS-QP2010, Shimadzu Corp. Co., Ltd.) and gas chromatograph (G-2800T, Yanaco Analytical Systems Inc.) after gaseous hydrogen fluoride and fluorine gas were removed by passing through a tube filled with NaF pellets (Morita Chemical Industries, 99.9%) and activated alumina balls. Porapak-R and Molecular Sieve 5A were used as column packings. Helium was used as a carrier gas.

3. Results and discussion

3.1. Anodic behavior of metal fluorides added carbon anodes

In order to optimize the conditions for pre-electrolysis, the anodic behavior of the MgF_2/C and CaF_2/C were investigated by cyclic voltammetry. Fig. 1 shows anodic polarization curves of MgF_2/C and CaF_2/C in molten $\text{NH}_4\text{F-KF-3HF}$ at 100°C and at a sweep rate of 100 mV s^{-1} . In the first anodic sweep, a small peak was observed at 1.8 V, which is due to the electrolysis of residual water in the melt, i.e., the formation of graphite oxide, $\text{C}_2\text{O}(\text{OH})_y$, oxygen, and/or small amount of fluorine-GICs having semi-covalent C–F bonds. It was followed by a plateau up to 4 V, where fluorine-GICs having semi-covalent C–F bonds, $(\text{C}_x\text{F})_n$ ($x > 3$), with a higher surface energy and a higher electric conductivity were formed [2–14]. The anodic current increased from 4.0 V, where the discharge of fluoride ions took place. After peaking at 6.5–7.0 V, the current decreased acutely because of the occurrence of the anode effect, where insulating graphite fluoride with covalent C–F bonds, $(\text{CF})_n$ having an extremely low surface energy was formed on the carbon surface [2–5]. The peak current density at 6.5–7.0 V on the MgF_2/C anode was higher than that on the CaF_2/C anode, so that we gave priority to former anode in following sections. Significant changes were observed in the second sweeps. The peak and plateau in the potential range of 1.8–4.0 V disappeared and the current due to the discharge of fluoride ions started to flow at potentials higher than 5.0 V. A rapid decrease in current was also observed at potentials higher than ca. 6.5 V.

From these results, it is concluded that the anodic reactions on metal fluoride added carbon anode can be divided into four regions: electrolytic oxidation of water in the melt (Region I), formation of a fluorine-GIC film (Regions I and II), electrochemical fluorination of ammonium cations and/or ammonia on the carbon anode covered with a fluorine-GIC film (Region III), and the occurrence of the anode effect (Region IV). These results agreed with the results in a previous report on LiF impregnated carbon anode [27].

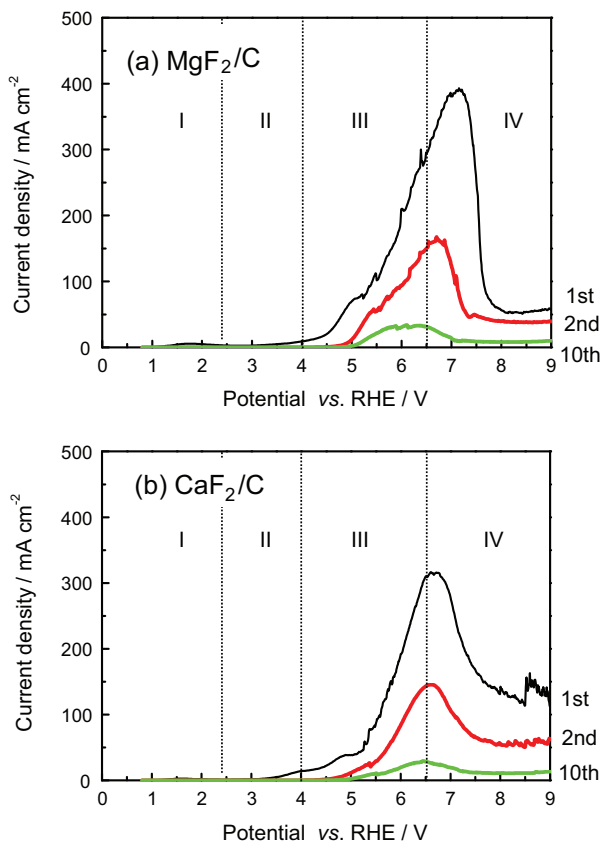


Fig. 1. Anodic polarization curves of (a) MgF_2 and (b) CaF_2 added carbon anodes in molten $\text{NH}_4\text{F}\cdot\text{KF}\cdot 3\text{HF}$ at 100°C and at a sweep rate of 100 mV s^{-1} .

3.2. Formation of fluorine-GICs on graphite sheet anodes in $\text{NH}_4\text{F}\cdot\text{KF}\cdot 3\text{HF}$ melts containing metal fluorides

In order to investigate the catalytic effect of metal fluorides on GIC formation in detail, a graphite sheet anode was used as a model anode in molten $\text{NH}_4\text{F}\cdot\text{KF}\cdot 3\text{HF}$ containing a colloidal suspension of metal fluorides and those anodes after electrolysis were analyzed by XRD. The potential dependence on fluorine-GIC formation was investigated on the graphite sheet anode. Fig. 2 shows XRD patterns of graphite sheet anodes after potentiostatic electrolysis at 2.3, 4.0, 6.0, and 8.0 V for 500 C cm^{-2} in molten $\text{NH}_4\text{F}\cdot\text{KF}\cdot 3\text{HF}$ containing 1 wt.% MgF_2 and CaF_2 at 100°C . The stage number, n , was determined from the c -axis repeat distance of fluorine-GICs, l_c , using the following equation [34]:

$$l_c \text{ (nm)} = 0.605 + 0.335(n - 1), \quad (1)$$

The diffraction lines at $2\theta = 26.5^\circ$ and 54.7° , which are assigned to hexagonal graphite (002) and (004) planes [27], were commonly observed for all samples. On the samples after kept at 2.3 V (Region II) in both electrolytes, additional diffraction lines assigned to fluorine-GICs were observed at $2\theta = 22.5^\circ$, 34.06° , 37.92° , 40.82° , 50.8° , and 53.86° , which are assigned to (007), (0010), (0011), (0012), (0015), and (0016) planes, respectively, of stage-7 fluorine-GIC [27]. In contrast, these lines were not observed after kept at 4.0, 6.0 (Region III), and 8.0 V (Region IV). The other small diffraction lines were attributed to the residue of molten $\text{NH}_4\text{F}\cdot\text{KF}\cdot 3\text{HF}$. These results suggest that the stage number of fluorine-GIC depends on anode potential and that the graphite sheet anode should be polarized in Region II to enhance the formation of the fluorine-GICs.

In order to investigate the effect of charge passed on the formation of fluorine-GICs, electrolysis was conducted at 2.3 V for 100 and

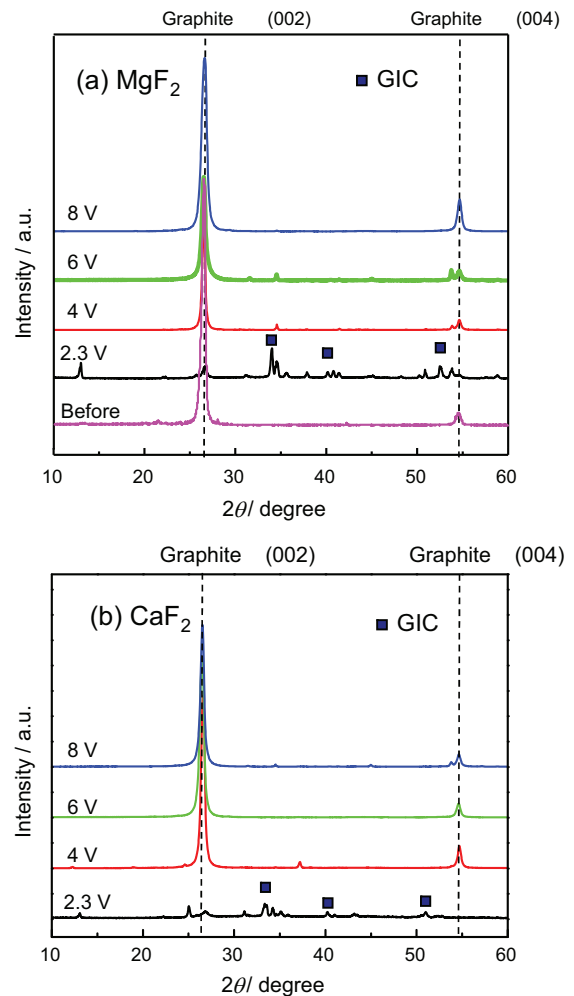


Fig. 2. X-ray diffraction patterns of the graphite sheet anodes before and after potentiostatic electrolysis for 500 C cm^{-2} in molten $\text{NH}_4\text{F}\cdot\text{KF}\cdot 3\text{HF}$ containing 1 wt.% (a) MgF_2 and (b) CaF_2 at 100°C .

500 C cm^{-2} in the melt containing 1 wt.% MgF_2 with a graphite sheet anode. Fig. 3(a) and (b) shows XRD patterns of the graphite sheet anode after electrolysis. The intensity of the diffraction from stage-7 fluorine-GICs increased with increasing charge passed. Further-

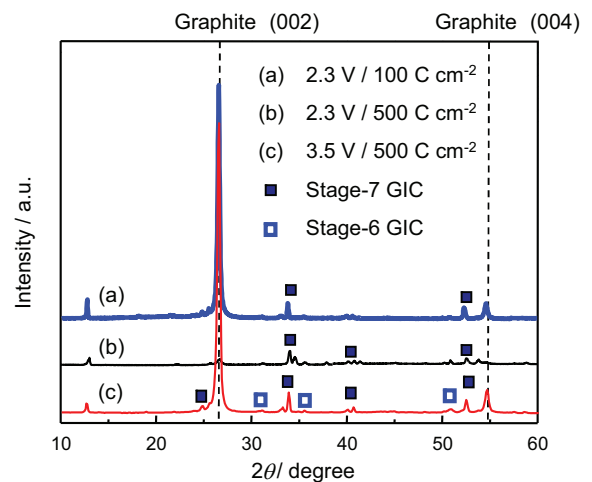


Fig. 3. X-ray diffraction patterns of the graphite sheet anodes after electrolysis at 2.3 V for (a) 100 C cm^{-2} and (b) 500 C cm^{-2} and (c) at 3.5 V for 500 C cm^{-2} in molten $\text{NH}_4\text{F}\cdot\text{KF}\cdot 3\text{HF}$ containing 1 wt.% MgF_2 at 100°C .

more, Fig. 3(c) shows X-ray diffraction pattern of the graphite sheet anode polarized at 3.5 V for 500 C cm^{-2} in molten $\text{NH}_4\text{F}\cdot\text{KF}\cdot 3\text{HF}$ containing 1 wt.% MgF_2 at 100°C . As shown in Fig. 3(c), diffraction lines observed at $2\theta = 31.0^\circ$, 35.4° , and 50.8° are assigned to (008), (009), and (0013) planes, respectively, of stage-6 fluorine-GIC [27]. In addition, weak diffraction line at around $2\theta = 12.6^\circ$, which is assigned to (003) plane of stage-7 fluorine-GIC and/or (004) plane of stage-6 fluorine-GIC, respectively, of stage-7 fluorine-GIC were commonly observed. These results mean that higher potentials in Region II accelerate formation of fluorine-GICs on the surface, which gives a fluorine-GIC with a lower stage number.

3.3. Surface analysis of MgF_2 added carbon anode after pre-electrolysis

MgF_2/C anodes were polarized at 3.5 V for 500 C cm^{-2} as pre-electrolysis in molten $\text{NH}_4\text{F}\cdot\text{KF}\cdot 4\text{HF}$ at 100°C , and the pre-electrolyzed surfaces were analyzed by XPS and XRD. Fig. 4 shows XPS spectra of the C 1s and F 1s levels of the MgF_2/C anode after the pre-electrolysis. A large peak at 284.5 eV and a shoulder at ca. 286 eV were observed on the C 1s spectrum. They can be divided in four symmetrical peaks at 284.8, 285.8, 288.0 and 289.5 eV, which is denoted as C_1 , C_2 , C_3 , and C_4 , respectively, as shown in the upper panel of Fig. 4 [35,36]. The binding energy and the full width at half maximum (FWHM) of every component are shown in Table 1. The C_1 peak at 284.8 eV is assigned to the C–C bonds of the graphite bulk and the C_2 peak at 285.8 eV to the C–O and/or C–H bonds, which was present even on the original graphite before pre-electrolysis. Peak C_3 at 288.0 eV and peak C_4 at 289.5 eV are assigned to semi-covalent C–F bonds and the covalent C–F bonds of graphite fluorides, respectively, which were formed during the pre-electrolysis. The peaks at 294 and 297 eV are assigned to $\text{K } 2p_{3/2}$ and $\text{K } 2p_{1/2}$, respectively, from the residue of the melt. On the other hand, a large peak appeared at ca. 687 eV on the F 1s spectrum and it can be divided in two symmetrical peaks at 686.7 and 688.1 eV. The former and latter peaks are assigned to the semi-covalent (F_1) and the covalent C–F bonds (F_2), respectively. These results revealed that fluorine-GICs were produced during pre-electrolysis at 3.5 V, together with a smaller amount of graphite fluoride.

Fig. 5 compares X-ray diffraction patterns of MgF_2/C anodes before and after pre-electrolysis at 3.5 V. Two broad diffraction lines were observed at $2\theta = 25^\circ$ and 43° and are assigned to the graphite (002) and (10) planes, respectively [37–39]. Some sharp diffraction lines observed at $2\theta = 27.4^\circ$, 35.4° , 40.6° , 43.9° , 53.7° , and 56.4° , are assigned to the (110), (101), (111), (210), and (220) planes, respectively, of MgF_2 in the carbon anode. The diffraction lines also observed at $2\theta = 34.9^\circ$, 38.6° , and 45.7° are assigned to (009), (0010), and (0012) planes, respectively, of stage-6 fluorine-GIC [27]. The results obtained by XRD are in accordance with those by XPS. From these results, it is concluded that the addition of MgF_2 , not only in the melt, but also in the carbon anode effectively catalyzes the formation of fluorine-GICs during the pre-electrolysis at 3.5 V.

Table 1

Binding energy (BE), full width at half maximum (FWHM), component and assignment of each peak separated from XPS spectra of C 1s and F 1s levels.

Component	BE (eV)	Assignment	$\text{MgF}_2/\text{C-PE}$ (Fig. 4)		$\text{MgF}_2/\text{C-PE-AE}$ (Fig. 9)	
			BE (eV)	FWHM (eV)	BE (eV)	FWHM (eV)
C1s						
C_1	284.8	C–C	284.8	1.57	284.7	1.41
C_2	285.8	C–O, C–H	285.8	1.48	285.8	1.72
C_3	288.0	Semi-ionic C–F bond	288.0	2.56	–	–
C_4	289.5	Covalent C–F bond	289.5	2.76	289.5	4.54
F1s						
F_1	686.7	Semi-ionic C–F bond	686.4	2.21	–	–
F_2	688.1	Covalent C–F bond	688.0	2.88	688.0	2.77

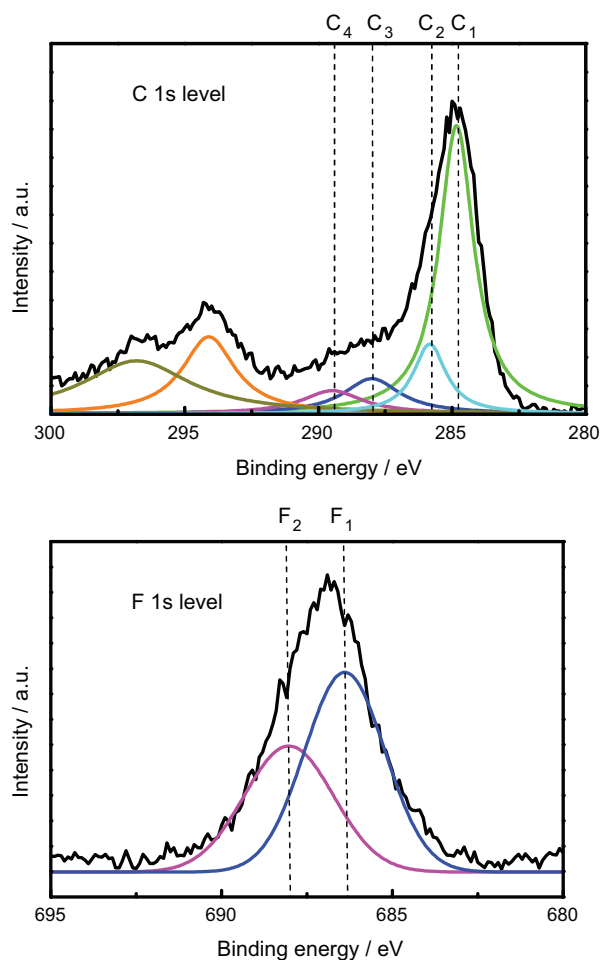


Fig. 4. XPS spectra of C 1s and F 1s level for the MgF_2/C anode polarized at 3.5 V for 500 C cm^{-2} in molten $\text{NH}_4\text{F}\cdot\text{KF}\cdot 4\text{HF}$ at 100°C ($\text{MgF}_2/\text{C-PE}$).

3.4. Effect of pre-electrolysis condition on critical current densities of MgF_2 added carbon anodes

To optimize the condition for pre-electrolysis of MgF_2/C anodes, CCDs on those were determined in molten $\text{NH}_4\text{F}\cdot\text{KF}\cdot 4\text{HF}$ at 100°C . The composition of electrolyte used in this section was slightly different from that in Sections 3.2 and 3.3. As the vapor pressure of HF over the $\text{NH}_4\text{F}\cdot\text{KF}\cdot 4\text{HF}$ melt is higher than that over the $\text{NH}_4\text{F}\cdot\text{KF}\cdot 3\text{HF}$ melt, the graphite sheet anode was completely expanded only after 30 C cm^{-2} by formation of fluorine-GICs and electrolysis was terminated [25]. Conversely, as the presence of KF in the melts reduces the current efficiency of NF_3 formation on the LiF impregnated carbon anode, it is considered that the $\text{NH}_4\text{F}\cdot\text{KF}\cdot 4\text{HF}$ melt is suitable for electrolytic synthesis of NF_3 . Fig. 6 shows galvanostatic polarization curves of a Pristine-C and MgF_2/C

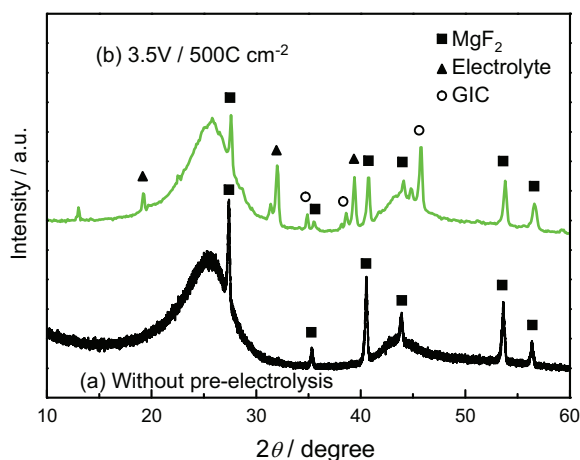


Fig. 5. X-ray diffraction patterns of MgF_2/C anodes (a) before pre-electrolysis and (b) after pre-electrolysis at 3.5 V for 500 C cm^{-2} in molten $\text{NH}_4\text{F}\cdot\text{KF}\cdot 4\text{HF}$ at 100 °C.

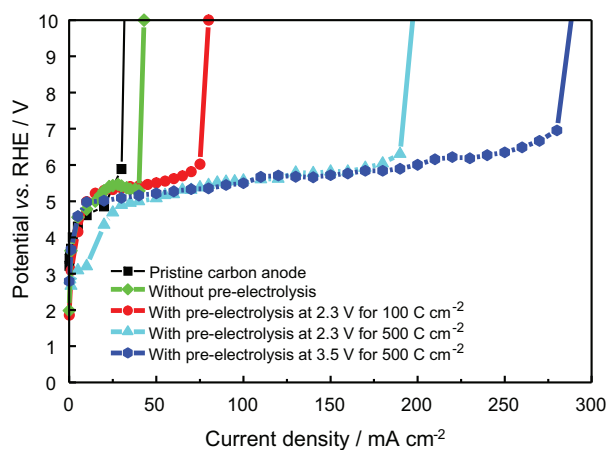


Fig. 6. Galvanostatic polarization curves of Pristine-C and MgF_2/C anodes with and without pre-electrolysis in molten $\text{NH}_4\text{F}\cdot\text{KF}\cdot 4\text{HF}$ at 100 °C.

anodes treated with and without pre-electrolysis under various conditions. The values of CCD obtained from the anodic polarization curves are summarized in Table 2 together with those found in the literature [17,18,20,22,27,28]. Without pre-electrolysis, the CCD on the MgF_2/C anode was 42 mA cm^{-2} , which was slightly higher than that of the Pristine-C anode (30 mA cm^{-2}). Pre-electrolysis at 2.3 V was effective for improving CCD, and CCD increased with increasing

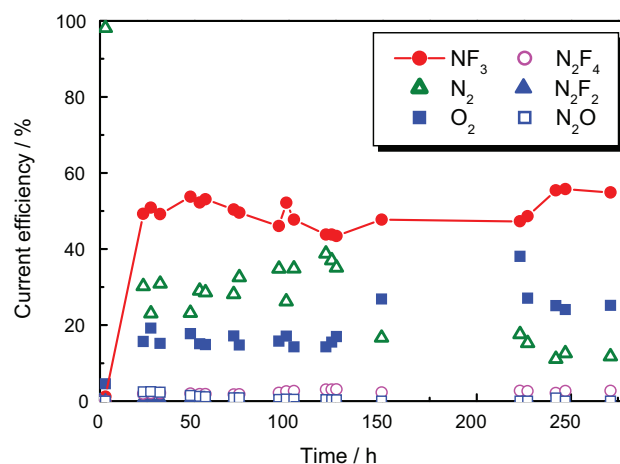


Fig. 7. Changes in current efficiencies for the constituents in anode gas with time on $\text{MgF}_2/\text{C}\text{-PE}$ anode at 100 mA cm^{-2} in molten $\text{NH}_4\text{F}\cdot\text{KF}\cdot 4\text{HF}$ at 100 °C.

charge passed, i.e., 75 mA cm^{-2} for 100 C cm^{-2} and 190 mA cm^{-2} for 500 C cm^{-2} . As shown in Fig. 3(a) and (b), the amount of stage-7 fluorine-GIC increased with increasing the charge passed for pre-electrolysis. Therefore, it is concluded that the charge passed during pre-electrolysis is one of the most important parameters for suppressing the anode effect.

Furthermore, pre-electrolysis at 3.5 V for 500 C cm^{-2} significantly increased CCD to 290 mA cm^{-2} on the MgF_2/C anode. This fact suggests that stage-6 fluorine-GIC was generated on the MgF_2/C anode by pre-electrolysis at 3.5 V similarly to the graphite sheet anode. As shown in Fig. 3(c), the amount of fluorine-GICs increased and the stage number of fluorine-GICs decreased with increasing the anode potential not less than 4.0 V for pre-electrolysis at a given charge passed. Therefore, it is concluded that the anode potential for pre-electrolysis is another important parameter for suppressing the anode effect and that best condition for pre-electrolysis in present study is at 3.5 V for 500 C cm^{-2} on the MgF_2/C anode.

3.5. Electrolytic production of NF_3 using $\text{MgF}_2/\text{C}\text{-PE}$

Since the electrolytic NF_3 production using nickel anode and fluorine (F_2) production using carbon anode are operated at 100 mA cm^{-2} in the industry, it is very important to develop carbon anodes that can maintain at least 100 mA cm^{-2} in the electrolytic production of NF_3 .

Table 2
Summary of CCDs in electrolytic production of NF_3 and F_2 .

Electrolyte	Anode	Pre-electrolysis	Stage number of GIC	CCD (mA cm^{-2})	References
$\text{NH}_4\text{F}\cdot\text{KF}\cdot 4\text{HF}$	Pristine carbon	–		30	[27]
		2.3 V/250 C		50	
		2.3 V/500 C		50	
		2.3 V/1000 C	7, 6	50	
		2.3 V/500 C, 4.0 V/500 C	5	122	
	LiF impregnated carbon	–		55	[24]
MgF_2 added carbon	–			42	Present study
	2.3 V/100 C	7	78		
	2.3 V/500 C	7	190		
	3.5 V/500 C	6	290		
KF·2HF	Pristine carbon	–		27	[21]
	LiF impregnated carbon	–		>60	
	LiF–NaF impregnated carbon	–		>60	[20]
	AlF_3 –NaF impregnated carbon	–		>60	
	LiF– CaF_2 added carbon	–		>40	[24]

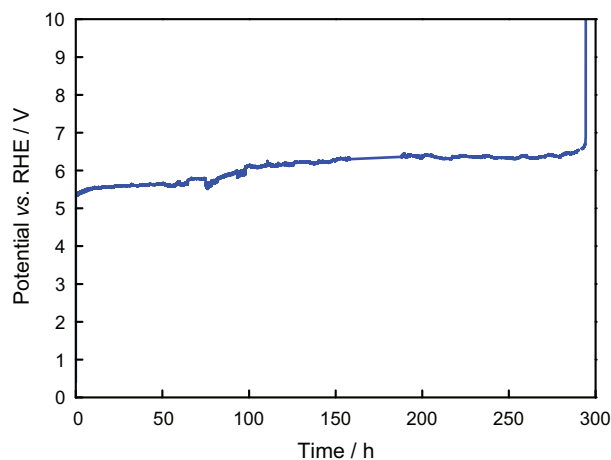


Fig. 8. Variation of the potential of MgF₂/C-PE anode during electrolysis at 100 mA cm⁻² in molten NH₄F·KF·4HF at 100 °C.

Electrolysis was carried out at 100 mA cm⁻² using the MgF₂/C anode with pre-electrolysis at 3.5 V for 500 C cm⁻² in molten NH₄F·KF·4HF at 100 °C (MgF₂/C-PE). Fig. 7 shows the changes in current efficiency for the constituents in the anode gas with time. The anode gas was composed of NF₃, N₂, O₂, N₂F₂, N₂F₄, and N₂O. Although N₂ gas was the main product in the beginning of electrolysis, the current efficiency for NF₃ formation increased with time, reached its maximum (55.5%) at ca. 50 h and then became almost constant. The maximum current efficiencies for NF₃ formation on Pristine-C [26], the MgF₂/C, and the MgF₂/C-PE are summarized in Table 3 together with the current efficiencies for other gaseous products. Although the current density on MgF₂/C-PE was ten times higher than those on Pristine-C and MgF₂/C, the current efficiency for NF₃ formation on the former was almost the same as those on the latter two.

Fig. 8 shows the variation of the anode potential during electrolysis at 100 mA cm⁻² using MgF₂/C-PE in molten NH₄F·KF·4HF at 100 °C. The anode potential was ca. 5.5 V for 50 h in the beginning, then increased gradually to 6.2 V, and stagnated at 6.2 V from 100 to 290 h. At 290 h, the anode potential rose suddenly up to over 10 V, where the anode effect took place and electrolysis was terminated. It is well known that the anode effect is enhanced in inadequately dehydrated melt [18]. It is not easy to eliminate sufficiently a trace of water in the melt containing fluorides such as NH₄F. Therefore, it is expected that electrolysis can be continued at 100 mA cm⁻² for longer duration without the anode effect, when well dehydrated (less than 0.006 wt% (ca. 6 mmol dm⁻³) [33]) melt is used as an electrolyte.

3.6. Surface analysis of MgF₂/C-PE-AE.

Fig. 9 shows XPS spectra of the C 1s and F 1s level of the MgF₂/C used in electrolysis for 300 h in Fig. 8 (MgF₂/C-PE-AE). The result of peak fitting and binding energy and the full width at half maximum (FWHM) of every component is shown in Table 1. Compared with XPS spectra for the pre-electrolyzed MgF₂/C anode before electrolysis (MgF₂/C-PE) in Fig. 4, the C₃ peak on the C 1s spectrum and the F₁ peak on the F 1s spectrum, which are assigned to the semi-covalent C–F bonds of fluorine-GICs, disappeared. These facts suggest that the layer of fluorine-GICs formed in pre-electrolysis changed to graphite fluoride with the covalent C–F bonds.

Fig. 10 shows X-ray diffraction pattern of the anode after electrolysis (MgF₂/C-PE-AE). When compared with the XRD pattern in Fig. 5, no diffraction line assigned to fluorine-GICs was observed. This fact well agrees with the results of the XPS anal-

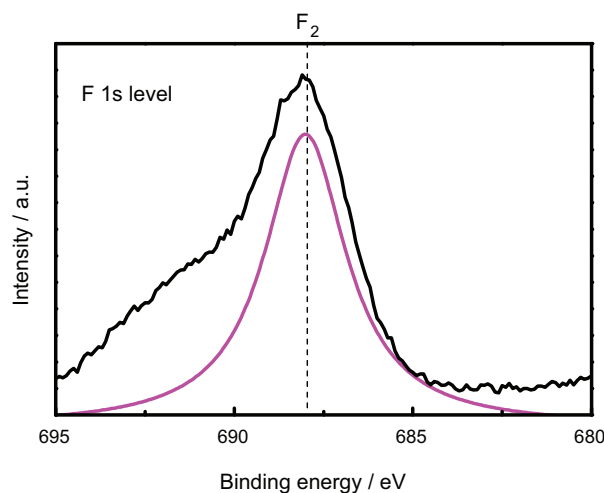
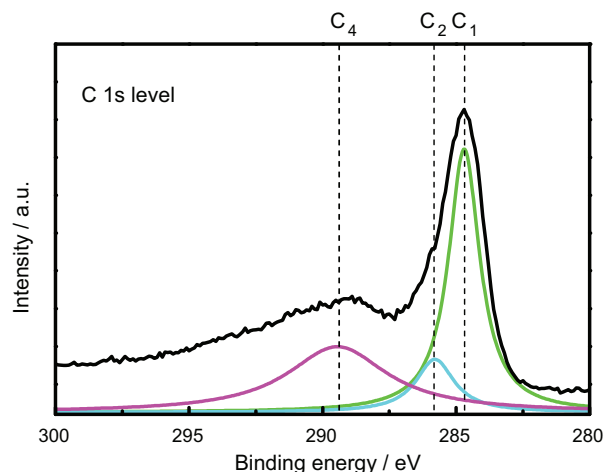


Fig. 9. XPS spectra of the MgF₂/C anode with pre-electrolysis at 3.5 V for 500 C cm⁻² after electrolysis at 100 mA cm⁻² for 300 h in molten NH₄F·KF·4HF at 100 °C (MgF₂/C-PE-AE).

ysis in Fig. 9. SEM images of MgF₂/C, MgF₂/C-PE, and MgF₂/C-PE-AE are shown in Fig. 11. The morphology of MgF₂/C was highly rugged and had many macropores, which are characteristic to an isotropic dense carbon. No significant difference appeared in the texture of

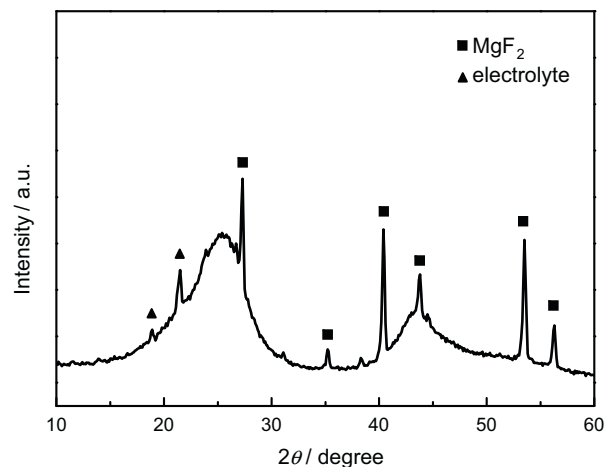
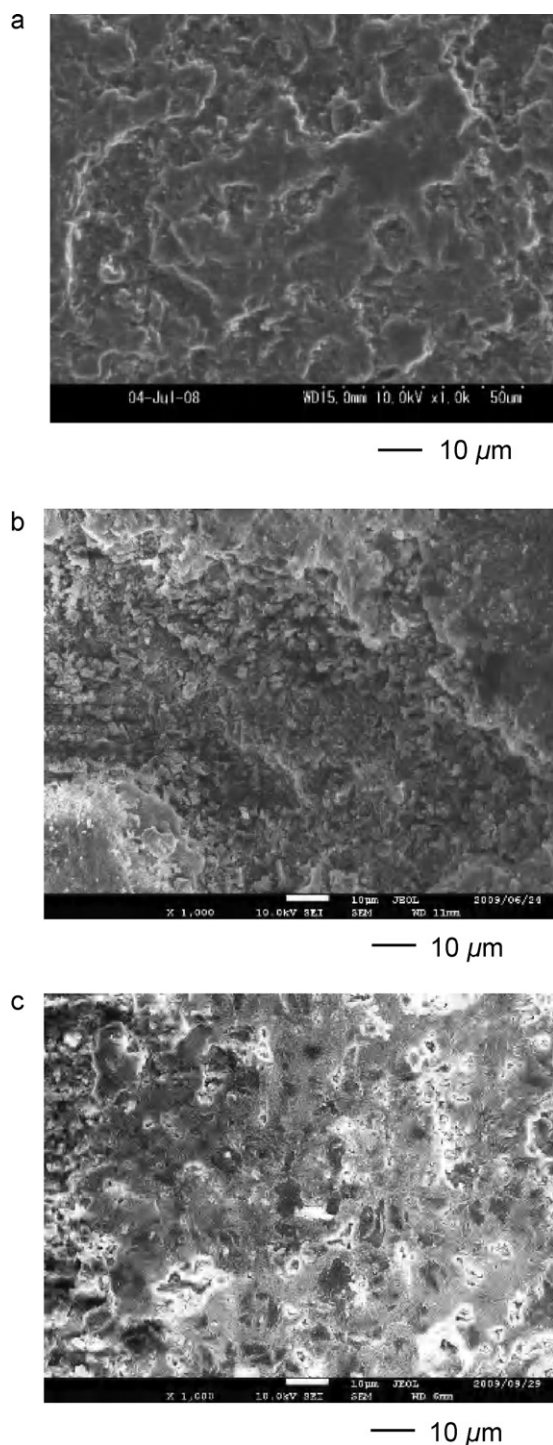


Fig. 10. X-ray diffraction patterns of MgF₂/C anode with pre-electrolysis at 3.5 V for 500 C cm⁻² after electrolysis at 100 mA cm⁻² for 300 h in a molten NH₄F·KF·4HF at 100 °C (MgF₂/C-PE-AE).

Table 3The current efficiencies for the constituents in the anode gas using various carbon anodes in molten $\text{NH}_4\text{F}\cdot\text{KF}\cdot 4\text{HF}$ at 100 °C.

Anode material	Current density (mA cm^{-2})	Current efficiency (%)						Overall
		N_2	O_2	NF_3	N_2F_2	N_2F_4	N_2O	
Pristine carbon [26] (Pristine-C)	10	23.6	8.22	51.4	3.51	4.56	3.15	94.4
MgF_2 added carbon without pre-electrolysis [26] (MgF_2/C)	10	28.0	8.28	53.2	1.62	3.27	1.51	96.0
MgF_2 added carbon with pre-electrolysis ($\text{MgF}_2/\text{C-PE}$)	100	12.6	24.1	55.7	0.12	2.64	0	95.2

**Fig. 11.** SEM images of MgF_2/C anodes (a) without pre-electrolysis and with pre-electrolysis at 3.5 V for 500 C cm^{-2} (b) before ($\text{MgF}_2/\text{C-PE}$) and (c) after electrolysis at 100 mA cm^{-2} for 300 h in a molten $\text{NH}_4\text{F}\cdot\text{KF}\cdot 4\text{HF}$ at 100 °C ($\text{MgF}_2/\text{C-PE-AE}$).

the carbon surface after pre-electrolysis as shown in Fig. 11(b). In contrast, the surface morphology of $\text{MgF}_2/\text{C-PE-AE}$ was characterized by shiny mirror-like surface, as shown in Fig. 11(c). Groult et al. have reported that activation of carbon at 40 V in $\text{KF}\cdot 2\text{HF}$ modified strongly the surface morphology by electropolishing with sparks and heat [13,14]. Based on this fact, it is considered that smoothing and cleaning of the anode surface may be induced by occurrence of the anode effect.

4. Conclusions

Metal fluoride added carbon anodes treated by pre-electrolysis were investigated for electrolytic production of nitrogen trifluoride (NF_3) in molten $\text{NH}_4\text{F}\cdot\text{KF}\cdot 4\text{HF}$ at 100 °C. The conditions for pre-electrolysis were first optimized using a graphite sheet anode as a model anode. The formation of fluorine-graphite intercalation compounds (fluorine-GICs) with semi-covalent C–F bonds, $(\text{C}_x\text{F})_n$, on the MgF_2 and CaF_2 added carbon anode surface was accelerated by pre-electrolysis at potentials less than 4.0 V. The stage number of fluorine-GICs was dependent on the condition of electrolysis such as charge passed and anode potential, and was gradually decreased with the increase in charge passed. Critical current densities (CCD) on the MgF_2 added carbon anodes pre-electrolyzed under various conditions were determined, and the highest CCD was 290 mA cm^{-2} obtained for that pre-electrolyzed at 3.5 V for 500 C cm^{-2} . This anode was successfully used in the electrolysis at 100 mA cm^{-2} for 290 h and the maximum NF_3 current efficiency was 55%. The anode effect took place after electrolysis for 290 h, because a trace of water in the melt enhanced formation of the $(\text{CF})_n$ layer. From these results, it was concluded that the metal fluoride added carbon anode treated by pre-electrolysis has a high potential for electrolytic production of NF_3 at high current densities.

Acknowledgments

This work was supported by a grant to the Research Center for Advanced Science and Technology at Doshisha University from the Ministry of Education, Japan and scholarship contribution of Mitsui Chemicals, Inc.

References

- [1] A. Tasaka, J. Fluorine Chem. 128 (2007) 296.
- [2] A. Tasaka, PhD Thesis, Kyoto University, 1970.
- [3] M. Nishimura, A. Tasaka, K. Nakanishi, N. Watanabe, *Denki Kagaku (Electrochemistry)* 38 (1970) 294.
- [4] A. Tasaka, N. Watanabe, *Yoyu-en (Molten Salts)* 13 (1970) 152.
- [5] H. Groult, S. Durand-Vidal, D. Devilliers, F. Lantelme, J. Fluorine Chem. 107 (2001) 247.
- [6] H. Groult, J. Fluorine Chem. 119 (2003) 173.
- [7] H. Groult, D. Devilliers, M. Vogler, C. Hinnen, P. Marcus, F. Nicolas, *Electrochim. Acta* 38 (1993) 2413.
- [8] H. Groult, D. Devilliers, S. Durand-Vidal, F. Nicolas, M. Combet, *Electrochim. Acta* 44 (1999) 2793.
- [9] H. Touhara, F. Okino, *Carbon* 38 (2000) 241.
- [10] A. Tasaka, H. Itoh, T. Isogai, H. Aio, T. Tojo, *J. Electrochem. Soc.* 138 (1991) 421.
- [11] H. Groult, D. Devilliers, M. Vogler, M. Chemla, *J. Appl. Electrochem.* 24 (1994) 870.
- [12] H. Groult, D. Devilliers, *J. Fluorine Chem.* 87 (1998) 151.

- [13] H. Groult, F. Lantelme, I. Crassous, C. Labrugère, A. Tressaud, C. Belhomme, A. Colisson, B. Morel, *J. Electrochem. Soc.* 154 (2007) C331.
- [14] I. Crassous, H. Groult, F. Lantelme, D. Devilliers, A. Tressaud, C. Labrugère, M. Dubois, C. Belhomme, A. Colisson, B. Morel, *J. Fluorine Chem.* 130 (2009) 1080.
- [15] T. Nakajima, in: T. Nakajima (Ed.), *Fluorine–Carbon and Fluoride–Carbon Materials, Chemistry, Physics and Application*, Marcel Dekker Inc., New York, USA, 1995, p. 3.
- [16] N. Watanabe, M. Ishii, S. Yoshizawa, *J. Electrochem. Soc. Jpn.* 29 (1961) 117.
- [17] D. Devilliers, B. Teisseyre, M. Chemla, *Electrochim. Acta* 35 (1990) 153.
- [18] T. Nakajima, T. Ogawa, N. Watanabe, *J. Electrochem. Soc.* 134 (1987) 8.
- [19] T. Tojo, J. Hiraiwa, M. Dohi, Y. Chong, N. Watanabe, *J. Fluorine Chem.* 54 (1991) 136.
- [20] T. Tojo, J. Hiraiwa, M. Dohi, Y. Chong, *J. Fluorine Chem.* 57 (1992) 93.
- [21] T. Tojo, J. Hiraiwa, N. Watanabe, *Kagaku Denki (Electrochemistry)* 66 (1998) 563.
- [22] H. Takebayashi, J. Hiraiwa, T. Tojo, A. Tasaka, N. Watanabe, *Yoyuen (Molten Salts)* 46 (2003) 51.
- [23] T. Tojo, *Yoyuen (Molten Salts)* 48 (2005) 28.
- [24] N. Watanabe, Y.-B. Chong, M. Aritsuka, M. Kanemaru, J. Mikami, *Proceedings of the 4th Japan–China Bilateral Conference on Molten Salt Chemistry and Technology*, Kyoto, Japan, November 8–13, 1992, p. 111.
- [25] A. Tasaka, T. Kawagoe, A. Takuwa, M. Yamanaka, T. Tojo, M. Aritsuka, *J. Electrochem. Soc.* 145 (1998) 1160.
- [26] A. Tasaka, M. Kodama, T. Tojo, H. Takebayashi, M. Inaba, *Abstract of International Conference on Fluorine Chemistry'04* Kyoto, Kyoto, Japan, May 9–11, 2004, p. 63.
- [27] A. Tasaka, M. Yamanaka (Miki), E. Morimoto, S. Nagamine, A. Mimoto, T. Fujukawa, M. Abe, A. Kobayashi, H. Takebayashi, T. Tojo, M. Inaba, *J. New Mat. Electrochem. Syst.* 9 (2006) 297.
- [28] A. Tasaka, *Electrochemistry* 75 (2007) 934.
- [29] A. Tasaka, H. Kobayashi, M. Negami, M. Hori, T. Osada, K. Nagasaki, T. Ozaki, H. Nakayama, K. Katamura, *J. Electrochem. Soc.* 144 (1997) 192.
- [30] Y. Shodai, M. Inaba, K. Momota, T. Kimura, A. Tasaka, *Electrochim. Acta* 49 (2004) 2131.
- [31] A. Tasaka, K. Mizuno, A. Kamata, K. Miki, *J. Fluorine Chem.* 57 (1992) 121.
- [32] A. Mimoto, T. Miyazaki, J. Yamashita, S. Nagamine, M. Inaba, A. Tasaka, *J. Electrochem. Soc.* 153 (2006) D149.
- [33] A. Tasaka, M. Hori, H. Harada, H. Inoue, M. Ohashi, *Sci. Eng. Rev. Doshisha Univ.* 34 (1993) 153.
- [34] T. Mallouk, N. Bartlett, *J. Chem. Soc. Chem. Commn.* (1983) 103.
- [35] A. Tressaud, E. Durand, C. Labrugere, *J. Fluorine Chem.* 125 (2004) 1639.
- [36] T. Nakajima, in: T. Nakajima (Ed.), *Fluorine–Carbon and Fluoride–Carbon Materials, Chemistry, Physics and Application*, Marcel Dekker Inc., New York, USA, 1995, p. 14.
- [37] T. Nakajima, M. Molinier, M. Motoyama, *Carbon* 29 (1991) 429.
- [38] J.M. Jiménez Mateos, E. Romero, C. Gómez De Salazar, *Carbon* 31 (1993) 1159.
- [39] Y. Sato, T. Kume, R. Hagiwara, Y. Ito, *Carbon* 41 (2003) 351.